

Climate Change Impact on Reservoir Performance Indexes in Agricultural Water Supply

Parisa Sadat Ashofteh¹; Omid Bozorg Haddad²; and Miguel A. Mariño, Dist.M.ASCE³

Abstract: This paper addresses the impact of climate change on the volume of inflow to a reservoir and the volume of downstream water demand by considering three climate change scenarios in an East Azerbaijan river basin. The HadCM3 model was used to estimate possible scenarios of temperature and rainfall for the period 2026–2039 under an emission scenario (A2). A hydrological model (IHACRES) was first calibrated for the basin; and then, a monthly time series of future temperatures and rainfall were entered into IHACRES. In addition, a 14-year time series of monthly runoff was simulated for 2026–2039. Modeling results indicated that the average long-term annual runoff volume decreased by 0.7% relative to the base period (1987–2000). However, by assuming a nonchanging cultivation area, the average long-term annual water demand volume for crops increased by 16%. Both simulation and optimization models of reservoir operation were used. The simulation of reservoir performance in the delivery of water demand was implemented according to the standard operating policy (SOP) and by using the water evaluation and planning (WEAP) model. The three aforementioned climate change scenarios were then introduced to the WEAP, and the reservoir performance indexes (reliability, vulnerability, and resiliency) were calculated. Results showed that indexes would change in the future relative to the base. Next, for the optimal operation of the reservoir with a water supply for agricultural and environmental purposes, the minimization of total squared deficiencies in the allocation to these purposes was determined for each month and climate change scenario by the using LINGO Version 11.0 software [nonlinear programming (NLP)] algorithm. Results showed that the indexes would change. DOI: 10.1061/(ASCE)IR.1943-4774.0000496. © 2013 American Society of Civil Engineers.

CE Database subject headings: Climate change; Reservoirs; Simulation; Optimization; Agriculture; Water supply.

Author keywords: Climate change; Operation management of reservoir; Reservoir performance indicators; Simulation; Optimization.

Introduction

Because of intensified human activity, growing population, and greenhouse gas emissions, most regions of the Earth are expected to experience significant increases in mean annual temperature ($>2^{\circ}\text{C}$) by the end of the present century [Intergovernmental Panel on Climate Change (IPCC) 2007]. The linear warming trend over the last 50 years (0.13°C per decade) is nearly twice that for the last 100 years. Studies of other climatological parameters, such as rainfall, cloudiness, and evaporation, have shown strongly varying trends on both global and regional scales (IPCC 2007). Without doubt, this phenomenon, called climate change, not only has been affecting climatic variables but also extreme events (e.g., droughts and floods), although it is not widely recognized (Robson 2002).

Several studies (Muzik 2001; Boyer et al. 2010) have shown that small perturbations in rainfall frequency and/or quantity can result in significant impacts on the mean annual discharge of rivers. Moreover, Christensen et al. (2004) indicated that modest changes in natural inflows result in larger changes in reservoir storage. Any changes in the hydrologic cycle will affect energy production and flood control measures (Xu and Singh 2004) to such an extent that water management adaptation measures will very likely be brought in. Anthropogenic climate change will affect water resources and agricultural consumption sectors in developing and developed countries. For example, in Iran, the agricultural sector is the primary water consumer and, thus, the study and evaluation of climate change impact on agricultural water supply is essential.

The common step that should be considered in all of these studies is climatic data simulation (such as temperature and rainfall) for the future. The most reliable and common instruments for obtaining projections of future global climate change are the fully coupled atmospheric-ocean general circulation models (AOGCMs) (Wilby and Harris 2006). According to their needs, investigators use a single general circulation model (GCM) or multiple models. On the other hand, investigations that examine the impacts of climate change show that these studies are mostly limited to assessing the effects of an upstream dam (water resources) or a downstream demand (water consumptions) (Quinn et al. 2004; Steele et al. 2008; Knox et al. 2010; Boyer et al. 2010). In contrast, climate change impact assessment and adaptation with the negative effects of this phenomenon emphasize the involvement of stakeholders in the framework of integrated water resources management (IWRM). Purkey et al. (2007) reported on the application of the water evaluation and planning model (WEAP) in the Sacramento River basin to study the impact of climate change on agricultural water management and its potential for adaptation. The WEAP model

¹Ph.D. Candidate, Dept. of Irrigation and Reclamation, Faculty of Agricultural Engineering and Technology, College of Agriculture and Natural Resources, Univ. of Tehran, Karaj, Tehran, Iran (corresponding author). E-mail: Pashofteh@ut.ac.ir

²Associate Professor, Dept. of Irrigation and Reclamation, Faculty of Agricultural Engineering and Technology, College of Agriculture and Natural Resources, Univ. of Tehran, Karaj, Tehran, Iran. E-mail: OBhaddad@ut.ac.ir

³Distinguished Professor Emeritus, Dept. of Land, Air and Water Resources, Dept. of Civil and Environmental Engineering, and Dept. of Biological and Agricultural Engineering, Univ. of California, 139 Veihmeyer Hall, Davis, CA 95616-8628. E-mail: MAMarino@ucdavis.edu

Note. This manuscript was submitted on February 19, 2012; approved on July 20, 2012; published online on July 27, 2012. Discussion period open until July 1, 2013; separate discussions must be submitted for individual papers. This paper is part of the *Journal of Irrigation and Drainage Engineering*, Vol. 139, No. 2, February 1, 2013. © ASCE, ISSN 0733-9437/2013/2-85-97/\$25.00.

includes a dynamically integrated rainfall-runoff hydrology module that generates the components of the hydrologic cycle from the input of a climatic time series. In the Sacramento River basin, four climate time series adopted for the 2006 climate change report were used to simulate agricultural water management without adaptation and with adaptation in terms of improvements in irrigation efficiency and shifts in cropping patterns during dry periods. The Geophysical Fluid Dynamics Laboratory (GFDL) and parallel climate model (PCM) were used under two greenhouse gas emission scenarios (A2 and B1). Results showed that an increase in temperature and a decrease in rainfall produced an increase in water demand. In addition, those adaptations resulted in lower overall water demands in the agricultural sector, to levels observed during the recent past, and associated reductions in groundwater pumping and increase in surface water allocations to other water use sectors. Raje and Mujumdar (2010) investigated climate change impact on multipurpose reservoir performance and derived adaptive policies for possible future scenarios. Climate change impacts on annual hydropower generation and four performance indexes (reliability with respect to three reservoir functions, viz. hydropower; irrigation and flood control; and resiliency, vulnerability, and deficit ratio with respect to hydropower) were studied. An optimal monthly operating policy was then derived by using stochastic dynamic programming (SDP) as an adaptive policy for mitigating the impacts of climate change on reservoir operation. Based on probabilistic changes in vegetation, changes to the irrigation rate were considered. Liu et al. (2010) investigated crop yield responses to climate change in the Huang-Huai-Hai plain of China. Results showed that a temperature increase of 2–5°C and a rainfall increase between 15 and 30% had a negative effect on crop yield. Boyer et al. (2010) considered the impact of climate change on the hydrology of St. Lawrence River tributaries. Projected river discharges for the next century for six climate series projections were generated with the hydrological model HSAMI. Three general circulation models (HadCM3, CSIRO-Mk2, and ECHAM4) and A2 and B2 emission scenarios were used to create a range of plausible scenarios. Results indicated a temperature increase in three future periods and a varied amount of discharge under climate change. Clearly, the impacts of climate change within a basin will affect the volume of river runoff and its monthly distribution, evapotranspiration, and water demand volume. Iran is not immune to climatic change impacts. Due to the

importance of agricultural production, the amount of water supply, its demand and distribution throughout the year are important. Thus, it is necessary to quantify reservoir performance indexes and estimate water demand and water availability in the future. The scope of previous investigations has been limited to the impact of individual or coupled parameters, such as temperature, rainfall, runoff, and water requirement, on reservoir management. This paper investigates the effect of the aforementioned parameters and presents a methodology for examining the behavior of a reservoir system, with emphasis on the impact of climate change on reservoir performance indexes.

For this study, temperature and rainfall data were extracted for the base period (1987–2000) and estimated for the future (2026–2039) by using the HadCM3 model under an A2 emission scenario. The impact of climate change was then investigated on the input runoff of the Aidoghmoush Reservoir in East Azerbaijan, by using the rainfall–runoff simulation model IHACRES for the future and also on the crop water requirement of the Aidoghmoush irrigation network. Subsequently, the volume of water demand downstream of the reservoir was calculated by considering the impact of three climate change scenarios on (1) runoff volume change; (2) demand volume change; and (3) changes in both volume of runoff and water demand. Next, the simulation of reservoir performance in the delivery of water demand based on input runoff to the river was carried out by using the WEAP model, and the reservoir performance indexes (reliability, vulnerability, and resiliency) were calculated. Finally, the optimal values of water release from the reservoir were determined by minimizing the total squared deficiencies in each month for the allocation of water under the aforementioned climate change scenarios by considering the performance indexes.

Methodology

This section discusses the processing of climatic data in a future period by using the HadCM3 model (under an A2 emission scenario), rainfall-runoff modeling, estimate of water demand volume, and simulation and optimization of reservoir performance under three climate change scenarios using the WEAP model and LINGO, respectively, and the calculation of performance indexes. Fig. 1 shows a flowchart of the methodology.

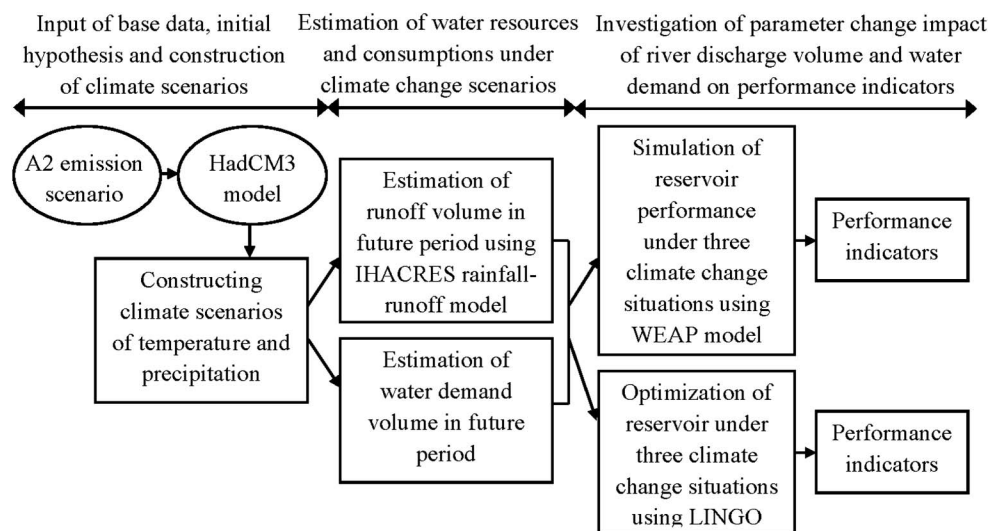


Fig. 1. Methodology

Construction of Climate Scenarios in Future Period

AOGCMs are the most comprehensive tools for estimating the response of the climate to radiative forcing. In 1996, a new set of emission scenarios, called *Special Report on Emission Scenario* (SRES), was presented by the IPCC. Each subscenario of SRES belongs to one of the A1, A2, B1, and B2 families. The A2 storyline and scenario family describes a very heterogeneous world. The underlying theme is self-reliance and preservation of local identities. Fertility patterns across regions converge very slowly, which results in a continuously increasing global population. Economic development is primarily regionally oriented, and per capita economic growth and technological changes are more fragmented and slower than in other storylines. One of the major problems with using an AOGCM model output is the large-scale of the computational grid (resolution) in terms of time and space relative to the study area. There are also techniques available for downscaling AOGCM outputs to the specific region or study area of interest. Climate change scenarios were spatially downscaled to the basin by using the “proportional” approach of each AOGCM. In this approach, information was obtained for the primary grid box for each model that the basin was within. A simple temporal downscaling approach, the “change fields” procedure, was used to develop the monthly climate scenarios for the basin. The climate scenarios were obtained by computing the differences (or ratio) between the averages of the AOGCM’s data set for the future and the corresponding averages of the models simulated for the base period. The changes for temperature are usually presented as differences, whereas for rainfall change, ratios are commonly used (Diaz-Nieto and Wilby 2005; Wilby and Harris 2006; Carter 2007). These processes are shown by the following equations:

$$\Delta T_i = (\bar{T}_{\text{AOGCM,fut},i} - \bar{T}_{\text{AOGCM,base},i}) \quad (1)$$

$$\Delta P_i = \left(\frac{\bar{P}_{\text{AOGCM,fut},i}}{\bar{P}_{\text{AOGCM,base},i}} \right) \quad (2)$$

where ΔT_i and ΔP_i = average long-term monthly temperature and rainfall change for month i , respectively; $\bar{T}_{\text{AOGCM,fut},i}$ and $\bar{P}_{\text{AOGCM,fut},i}$ = average long-term monthly temperature and rainfall for month i in the future simulated by AOGCM with related emission scenario, respectively; and $\bar{T}_{\text{AOGCM,base},i}$ and $\bar{P}_{\text{AOGCM,base},i}$ = average long-term monthly temperature and rainfall for month i in the base period simulated by AOGCM with related emission scenario, respectively. The temperature and rainfall changes that were determined by the GCM were then simply added to each month in the baseline time series (Wilby and Harris 2006). These processes can be represented by the following equations:

$$T_i = T_{\text{obs},i} + \Delta T_i \quad (3)$$

$$P_i = P_{\text{obs},i} \times \Delta P_i \quad (4)$$

where $T_{\text{obs},i}$ and $P_{\text{obs},i}$ = observed temperature and rainfall for month i , respectively; and T_i and P_i = temperature and rainfall time series for month i in the future, respectively.

Estimate of Water Resources and Consumptions under Climate Change

Rainfall-Runoff Simulation

The IHACRES module structure consists of a nonlinear loss module, which converts observed rainfall to effective rainfall or rainfall

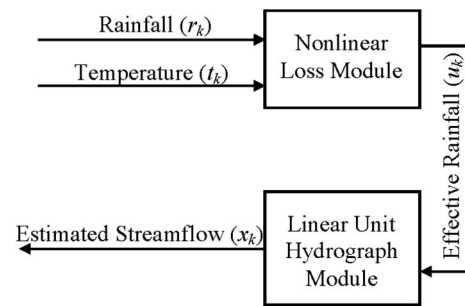


Fig. 2. Simulated rainfall runoff

excess, and a linear streamflow routing module, which extends the concept from unit hydrograph theory that the relationship between rainfall excess and total streamflow is conservative and linear (Jakeman and Hornberger 1993) (Fig. 2). The nonlinear loss module allows one to take into account the effect of antecedent weather conditions on the current status of the soil wetness index s_k and vegetation conditions and evapotranspiration effects. Here, the effective rainfall u_k is calculated from the measured temperature t_k and rainfall r_k by the recursive relations

$$s_k = c \cdot r_k + \left[1 - \frac{1}{\tau_w(t_k)} \right] s_{k-1} \quad (5)$$

$$u_k = r_k(s_k + s_{k-1})/2 \quad (6)$$

$$\tau_w(t_k) = \tau_w \exp[0.062f(t_r - t_k)] \quad (7)$$

where τ_r = reference temperature; c = constant calculated so that the volume of excess rainfall is equal to that of the total streamflow for the period over which the model is calibrated; τ_w and f = parameters that should be optimized; τ_w = time constant reflecting the rate of drying (in months) of the catchment at 25°C; and f = factor which modulates this rate as temperature varies.

The linear module allows any configuration of stores in parallel or series. In the two-store configuration, at time step k , quick flow, $x_k^{(q)}$, and slow flow, $x_k^{(s)}$, combine additively to yield streamflow (discharge), q_k :

$$q_k = x_k^{(q)} + x_k^{(s)} \quad (8)$$

with

$$x_k^q = -\alpha_q x_{k-1}^{(q)} + \beta_q u_k \quad (9)$$

$$x_k^s = -\alpha_s x_{k-1}^{(s)} + \beta_s u_k \quad (10)$$

where u_k = effective rainfall. Parameters α_q and α_s can be expressed as time constants for the quick and slow flow stores, respectively:

$$\tau_q = -\Delta / \ln(-\alpha_q) \quad (11)$$

$$\tau_s = -\Delta / \ln(-\alpha_s) \quad (12)$$

where Δ = time step (monthly here). In catchments that are modeled with only one store, only Eqs. (6) and (8) are relevant.

Estimate of Water Demand Volume in Reservoir Downstream

For calculating crop evapotranspiration, the reference crop evapotranspiration (by using the Penman-Monteith equation) and crop coefficient were used (Doorenbos and Pruitt 1984), according to the following equation:

$$ET_{C_t} = K_{C_t} \times ET_{0_t} \quad (13)$$

where ET_{C_t} = crop evapotranspiration in month t ; K_{C_t} = crop coefficient; and ET_{0_t} = reference crop evapotranspiration.

In addition, effective rainfall was calculated by using the Soil Conservation Service (SCS) method:

$$P_{\text{eff}_t} = P_t / 125 \times (125 - 0.2P_t) \quad P_t \leq 250 \text{ mm} \quad (14)$$

$$P_{\text{eff}_t} = 125 + 0.1 \times P_t \quad P_t > 250 \text{ mm} \quad (15)$$

where P_{eff_t} = average effective rainfall in month t ; and P_t = average rainfall in month t .

The net water requirement was then calculated with the equation

$$WR_t = ET_{C_t} - P_{\text{eff}_t} \quad (16)$$

where WR_t = net water requirement in month t . Next, the water demand volume was determined based on the constant area under cultivation:

$$V_t = \frac{WR_t \times 10 \times A}{1,000,000} \quad (17)$$

where V_t = water demand volume in month t ; and A = area under cultivation.

Land use/land cover was assumed to be constant over the entire period.

Reservoir Operation Models

Simulation Models

To simulate the operation of a reservoir, the standard operating policy (SOP) can be used. In the operation management of a reservoir based on SOP, if the total water in the reservoir is less than the monthly demand of consumer sectors, then the total water storage in the reservoir will be released, and there will be no storage for the next period. In this case, in the next period, only input discharge will supply consumers.

The WEAP model is a comprehensive, flexible, and user-friendly model for the planning and analysis of various scenarios that is able to simulate issues, such as water use patterns, costs, and water allocation patterns, river flow, groundwater resources, and water transmission lines. WEAP uses a water balance equation that is defined monthly for each node of the model (Sieber et al. 2005).

Optimization Models

Optimization models include the determination of the values of the decision variables pertinent to a decision-making problem so that a desired objective function is optimized. The objective function in problems of water allocation to agricultural and environmental purposes is defined as the minimization of the total squared deficiencies in each month. Thus, the objective function and constraints can be considered as

$$\text{Minimize } Def = \sum_{t=1}^n \left(\frac{D_t - R_t}{D_t} \right)^2 \quad (18)$$

subject to:

$$S_{t+1} = S_t + Q_t - R_t - SP_t - \frac{EV_t \times (aS_t + b)}{1,000} \quad (19)$$

$$S_{\min} \leq S_t \leq S_{\max} \quad (20)$$

$$0 \leq R_t \leq D_t \quad (21)$$

$$\begin{cases} SP_t = S_t + Q_t - \frac{EV_t \times (aS_t + b)}{1,000} - S_{\max} & \text{if } S_t + Q_t - \frac{EV_t \times (aS_t + b)}{1,000} \geq S_{\max} \\ SP_t = 0 & \text{otherwise} \end{cases} \quad (22)$$

where Def = objective function; D_t = agricultural and environmental demand in month t ; R_t = water release in month t ; S_t and S_{t+1} = storage volume of reservoir at the beginning and end of period t ; Q_t = inflow volume to reservoir in month t ; EV_t = evaporation height of reservoir in month t ; S_{\max} = total reservoir capacity; S_{\min} = dead volume of reservoir; SP_t = spill volume of reservoir in month t ; n = planning horizon; and a and b = constants whose values are obtained from a surface-volume curve so that $Ar_t = aS_t + b$ and Ar_t = area of reservoir in month t . In this study, to achieve the desired value of the objective function, inflow volume (runoff) and water demand volume need to be defined under climate change, with a constant evaporation volume in the future and with surface-volume curve constants. The optimal amounts of release and storage volumes of the reservoir can be determined by nonlinear programming (NLP) with LINGO.

Reservoir Performance Indexes

An important step in the application of optimization and simulation models for the operation of reservoirs is the use of performance indexes. This study uses reliability, resiliency, and vulnerability indexes (Loucks and Van Beek 2005).

The reliability of any time series can be defined as the number of data in a satisfactory state divided by the total number of data in the time series. By assuming satisfactory values in the time series X_t containing n values that are equal to or greater than some threshold X^T , then:

$$\text{Reliability } [X] = \frac{\text{number of time periods } t \text{ such that } X_t \geq X^T}{n} \quad (23)$$

The vulnerability is a measure of the extent of the differences between the threshold value and the unsatisfactory time series values. Clearly, this is a probabilistic measure. Some use expected values, some use maximum observed values, and others may assign a probability of exceedance to their vulnerability measures. By assuming an expected value, a measure of vulnerability should be used:

$$\begin{aligned} \text{Vulnerability } [X] &= \frac{\text{sum of positive values of } (X^T - X_t)}{\text{number of times an unsatisfactory value occurred}} \quad (24) \end{aligned}$$

The resiliency can be expressed as the probability that if a system is in an unsatisfactory state, the next state will be satisfactory. It is the probability of having an unsatisfactory value in any time period t . It can be calculated as:

$$\text{Resilience } [X] = \frac{[\text{number of times a satisfactory value follows an unsatisfactory value}]}{[\text{number of times an unsatisfactory value occurred}]} \quad (25)$$

Case Study and Definition of Scenarios

Study Area

The Aidoghmoush River, with a length of approximately 80 km, is the largest river in the Aidoghmoush Basin (drainage area = 1,802 km²) (Fig. 3). It originates in the northwest of Iran and traverses the east. The hydrometer gauging station Motorkhaneh, considered in this study, is located at the eastern end of the basin. The mean discharge at this gauging station and the mean yearly rainfall is 190×10^6 m³ per year and 378 mm, respectively. The monthly rainfall (from 10 stations), temperature (from 2 stations) and monthly discharge (from the hydrometer gauging station at Motorkhaneh) are available for the baseline period 1987–2000. The primary objectives of the project are river water regulation

with the construction of a dam and irrigation of the primary part of the dam downstream network. The network area is approximately 13,500 ha. Aidoghmoush Dam's normal level is 1,341.5 m above sea level, the total capacity, S_{\max} , is 145.7×10^6 m³, and the dead volume, S_{\min} , is 8.7×10^6 m³. Surface-volume curve constants a and b are 0.056 and 0.798, respectively.

Study Scenarios

In this study, simulation and optimization models for three climate change scenarios (impact of runoff volume change, impact of water demand volume change, and impact of changes in both volume of runoff and water demand) were simulated.

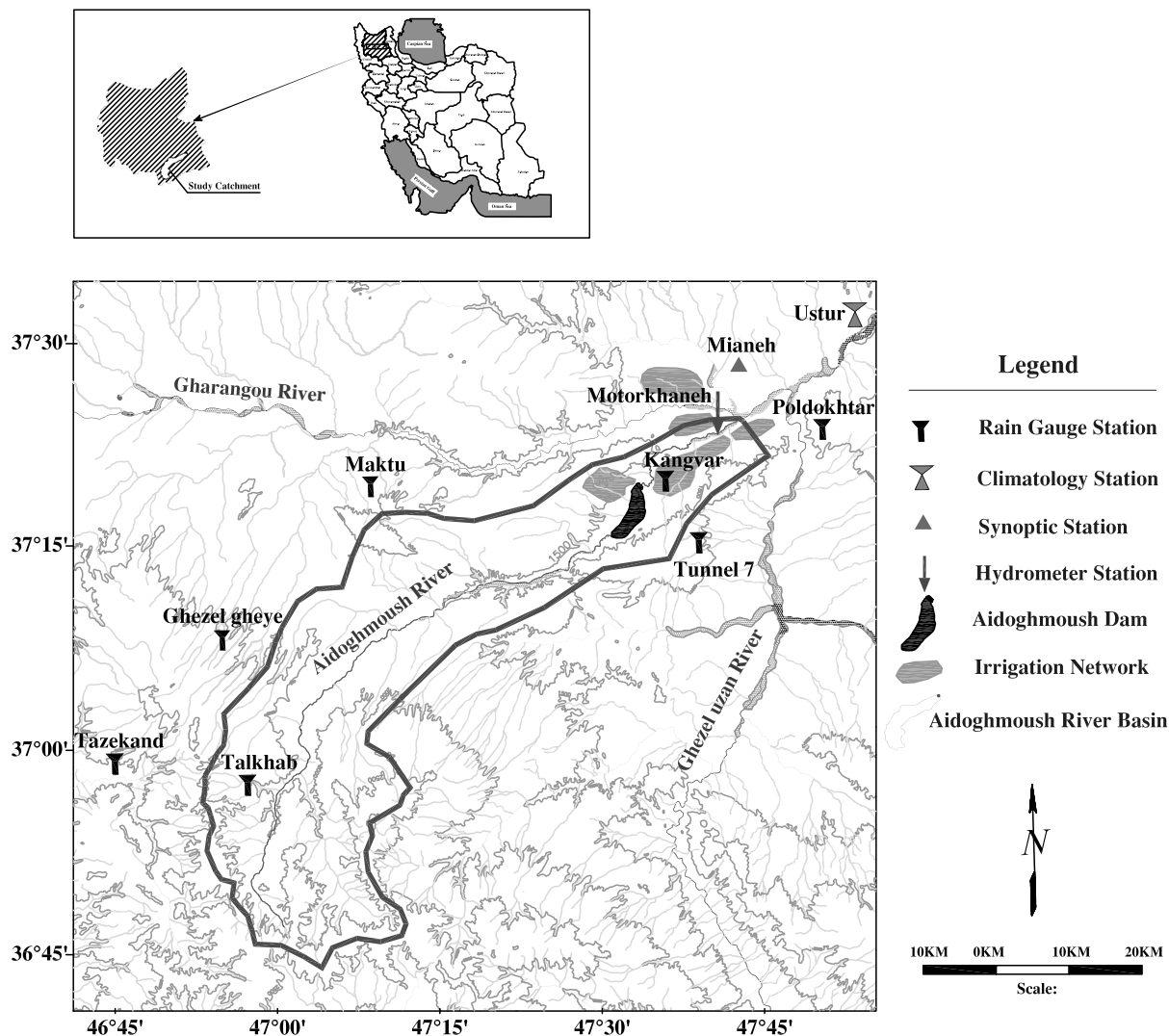


Fig. 3. Location of study basin and stations

Results

Investigation of Climate Model Performance for Base Period

This paper considered one GCM configuration, HadCM3 (IPCC-DDC 1998) under the A2 scenario, that had the best performance in the simulation for this case study. The 14-year average of monthly inflows were then calculated in the base period; and subsequently, those values were compared with the 14-year average of monthly observed temperature and rainfall (Fig. 4). As shown in the figure, HadCM3 yielded an estimated average temperature less than the observed data in most months whereas the performance of the model in simulating the rainfall was slightly weaker than the temperature. Next, the HadCM3 downscaling performance was tested by using three criteria: correlation coefficient, r ; root mean square error, RMSE; and mean absolute error, MAE (Table 1). As shown, HadCM3 simulated the climatic variables well.

Calculation of Climate Scenario for Future Period

The monthly temperature and rainfall time series of HadCM3 were downscaled under A2 for the future. Then, the average long-term monthly temperature and rainfall were calculated for the future period and base simulated period by the same model. Finally, using Eqs. (1) and (2), climate scenarios were calculated (Table 2). Results (Table 2) showed that the temperature increased (from

0.5 to 2.7°C) and the rainfall varied (−36–76%) in the future. The pattern of rainfall for the basin in the baseline was wintery. The time series of monthly temperature and rainfall were then calculated for the future by using Eqs. (3) and (4).

Investigation of Basin Runoff for Future Period

The IHACRES model was calibrated by using area-averaged monthly temperature and rainfall data from the basin and the Motorkhaneh monthly runoff data during 1987–2000. Different calibration and verification periods were tested by using the three previously mentioned criteria (“Results” section). The flow duration curve that shows the percentage of time that a given flow rate was equaled or exceeded is plotted for data sets of calibration and verification in Fig. 5. In this figure, the quality of calibration and verification data sets for the best result obtained from the fitted

Table 1. Performance Criteria of HadCM3 Models for Temperature and Rainfall Observed Data

| Climatic variable | Temperature | | | Rainfall | | |
|-------------------|-------------|-----------|----------|----------|-----------|----------|
| | r (%) | RMSE (°C) | MAE (°C) | r (%) | RMSE (mm) | MAE (mm) |
| HadCM3 model | 98.3 | 3.35 | 2.87 | 90.5 | 8.23 | 6.89 |

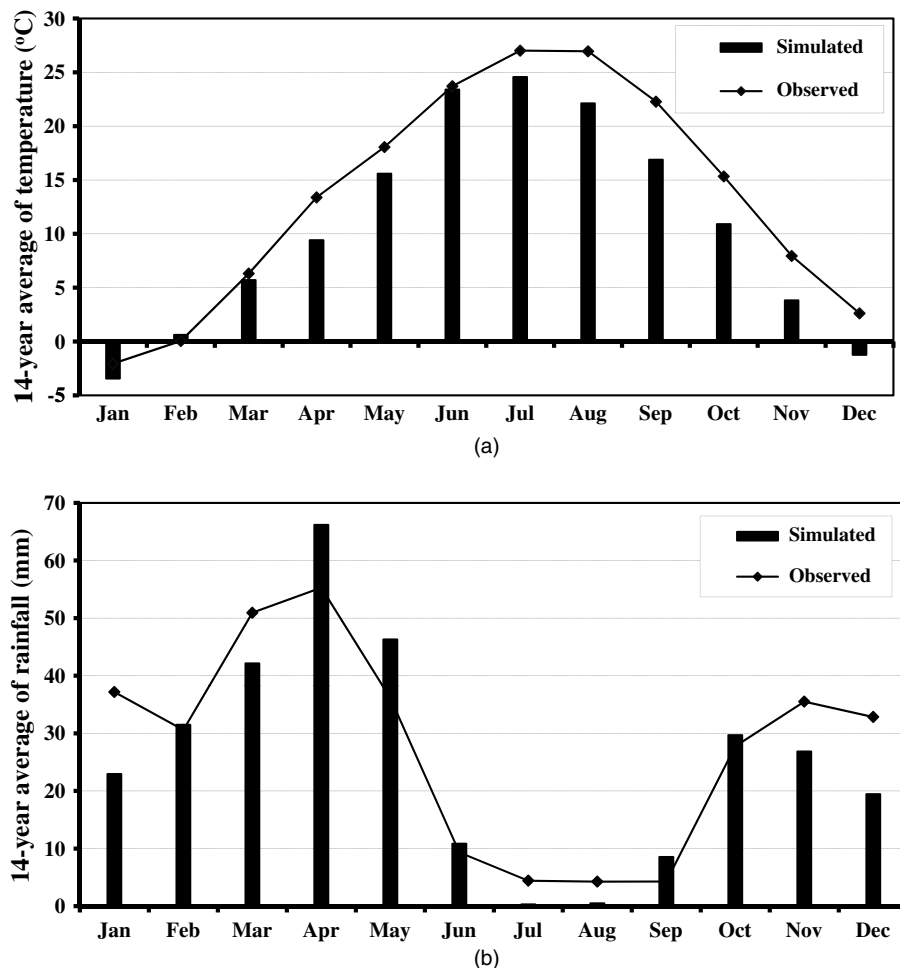


Fig. 4. 14-year monthly mean: (a) observed area averaged temperature; (b) rainfall data of the basin and HadCM3 model

Table 2. Climate Scenario of Temperature and Rainfall for HadCM3

| Climate scenario (change factor) | Month | | | | | | | | | | | |
|-------------------------------------|---------|----------|-------|--------|--------|--------|-------|--------|-----------|---------|----------|----------|
| | January | February | March | April | May | June | July | August | September | October | November | December |
| ΔP_i (%) | -8.69 | -6.19 | -1.22 | -26.22 | -20.94 | -35.97 | 76.32 | 4.67 | -21.35 | 36.50 | 9.82 | -1.82 |
| ΔT_i (°C) | 1.98 | 0.50 | 1.33 | 2.72 | 1.65 | 1.54 | 1.51 | 2.08 | 1.99 | 1.32 | 1.70 | 1.46 |

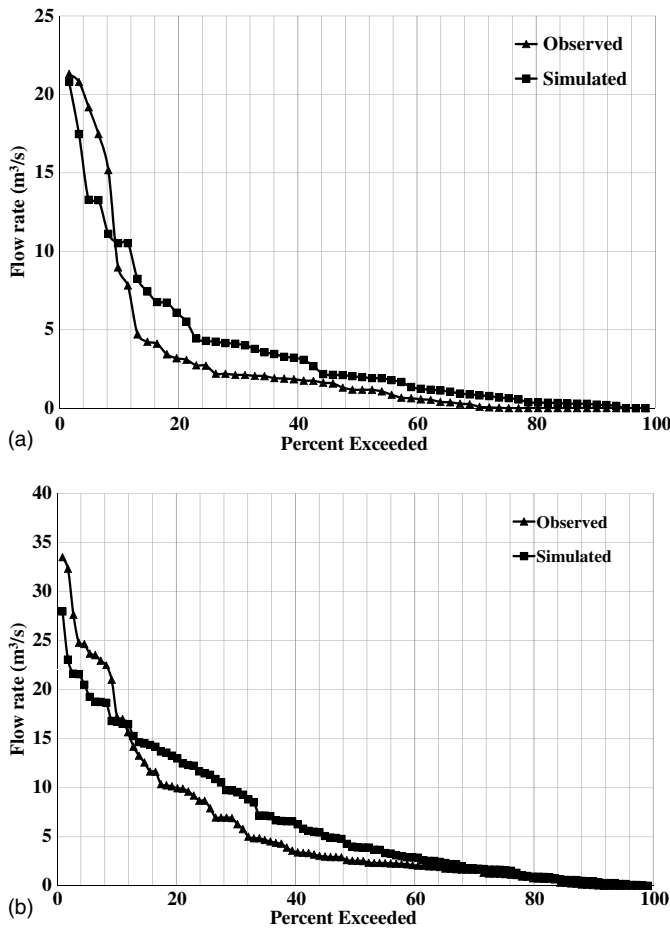


Fig. 5. Flow—duration curves of observed and simulated runoff: (a) calibration period ($r = 95\%$, $RMSE = 1.79 \text{ m}^3/\text{s}$, and $MAE = 1.32 \text{ m}^3/\text{s}$); (b) verification period ($r = 96\%$, $RMSE = 2.35 \text{ m}^3/\text{s}$, and $MAE = 1.71 \text{ m}^3/\text{s}$)

IHACRES model is presented. As it is clear from this figure, for a low flow rate (percent exceeded more than 60%), simulated and observed values are rather coincident over time. This issue is examined more in Table 3, which shows the volume comparison between the simulated and observed data for low, medium, and high flows. In water resource management studies, the sequence of inflow occurrences are of more importance. Thus, the time series of

the observed and simulated inflows should be presented as well. Fig. 6 shows the best results obtained from the calibration and verification of the IHACRES time series. The performance of the model in simulating the monthly runoff of the river was consistent. After the calibration and verification of the model, assuming that it was valid for the future, the time series of monthly temperature and rainfall in future were introduced into IHACRES, and the time series of monthly runoff was simulated for the future. Subsequently, the 14-year runoff for the base and future periods, respectively, was compared (Fig. 7). Results showed that the volume of runoff for the future decreased 0.7% ($0.09 \times 10^6 \text{ m}^3$) relative to the base (Table 4).

Calculation of Water Demand Volume under Climate Change

Given that all the necessary inputs for the calculation of water requirements for the future were not available, the relationship between temperature and reference evapotranspiration (ET_o) obtained from the base period data was used for the future period. In this regard, the regression method was used, and a regression relationship with $R^2 = 0.93$ was accepted. Next, this relationship was used to obtain ET_o for the future. To obtain relative humidity, its regression relationship with ET_o in the base period was used. Also, for wind speed, its amount for the base period was used. The value of K_c for every crop used in this study and for every month for the future period was calculated. By using the results of ET_o and K_c , the crop evapotranspiration of the basin was calculated for the future as well as the base period [Eq. (13)]. After a determination of effective rainfall, by using Eqs. (14) and (15) and the crop evapotranspiration from the previous step, the water requirement of crops for the future was determined by using Eq. (16), and water demand volume was calculated for each month according to Eq. (17). Fig. 8 shows a comparison of the annual volume of water demand for the base and future periods. The comparison of average long-term monthly volume of water demand in the aforementioned periods indicated that water demand volume increased in the future, showing a maximum increase in the summer (Fig. 9). In addition, Table 5 shows changes in water requirements and the volume of annual water demand in the future for the crops under consideration. According to these results, an average increase of 9–18% is expected in water requirements for different crops during the period 2026–2039. In some studies (e.g., Steinemann and Cavalcanti 2006), an increase of 10% in demand was introduced as a trigger for system stress. If this trigger were to be accepted here, there

Table 3. Volume Comparison Between Simulated and Observed Data for Low, Medium, and High Flows in Both Calibration and Verification Periods

| Period | Data | Inflow volume ($\times 10^6 \text{ m}^3$) | | |
|--------------|-----------|---|---|---------------------------------------|
| | | Low flow (percent exceeded > 60%) | Medium flow (40% < percent exceeded < 55%) | High flow (percent exceeded < 35%) |
| Calibration | Observed | 6.6 | 32.6 | 392.9 |
| | Simulated | 32.7 | 51.7 | 441.2 |
| Verification | Observed | 95.6 | 117.2 | 1,356.2 |
| | Simulated | 129.0 | 195.7 | 1,414.5 |

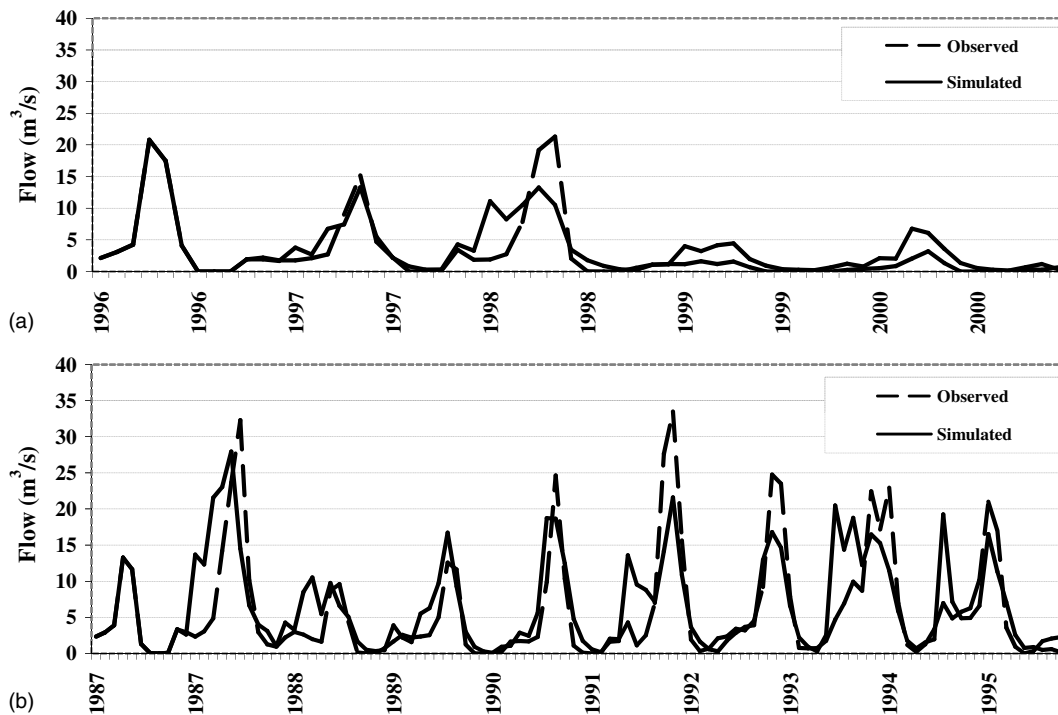


Fig. 6. Observed and modeled runoff: (a) calibration period ($r = 88\%$, $RMSE = 2.54 \text{ m}^3/\text{s}$, and $MAE = 1.42 \text{ m}^3/\text{s}$); (b) verification period ($r = 77\%$, $RMSE = 5.12 \text{ m}^3/\text{s}$, and $MAE = 3.19 \text{ m}^3/\text{s}$)

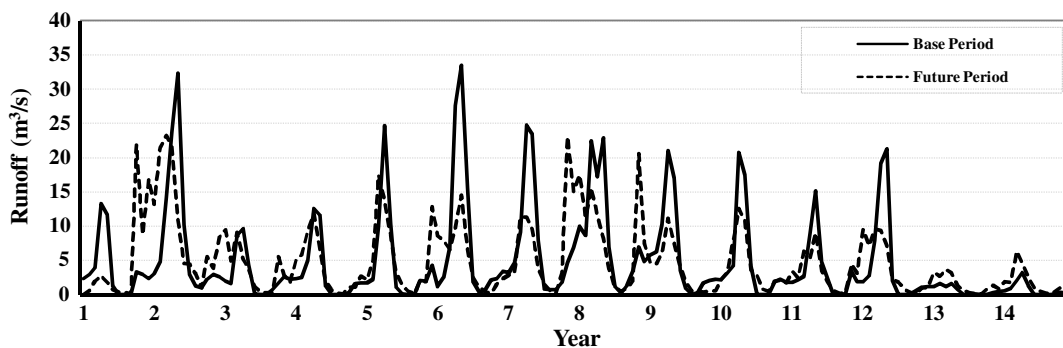


Fig. 7. Annual river runoff in base period and future

Table 4. Statistical Parameters of Annual Temperature, Rainfall, and Runoff Volume

| Statistical parameter | Rainfall (mm) | | Temperature (°C) | | Runoff volume ($\times 10^6 \text{ m}^3$) | |
|--------------------------|---------------|---------------|------------------|---------------|---|---------------|
| | Base period | Future period | Base period | Future period | Base period | Future period |
| Average | 27.37 | 26.08 | 13.47 | 15.11 | 12.55 | 12.46 |
| Standard deviation | 17.92 | 16.36 | 17.92 | 10.60 | 14.62 | 8.14 |
| Coefficient of variation | 65.49 | 62.75 | 133.10 | 70.13 | 116.47 | 65.32 |

would be stress in the system regarding the water requirement increase for all the crops except barley for the period 2026–2039. Climate change caused an increase in water demand volume for walnut, alfalfa, and potato crops in the amount of 9.56, 3.32, and $3.17 \times 10^6 \text{ m}^3$ per year, respectively, based on the existing area under cultivation (Table 5).

Simulation of Reservoir Performance under Climate Change Scenarios using WEAP

Three scenarios of climate change were considered in the WEAP, and results are presented in Fig. 10. Then, reliability, vulnerability, and resiliency indexes for each scenario for the base and future periods were used (Table 6). Because the water demand volume in the future increased 16% (from $112 \times 10^6 \text{ m}^3$ per year in the base to $130 \times 10^6 \text{ m}^3$ in future) and river runoff volume to the reservoir decreased 0.7% (from $12.55 \times 10^6 \text{ m}^3$ per year in the base to $12.46 \times 10^6 \text{ m}^3$ in future), the amount of water allocation, in terms of reservoir management based on the SOP, would be less than demand, assuming a 100% water supply. Similar calculations for 90 and 70% of water supply were derived, and results are shown in Fig. 10.

The results in Table 6 show that the reliability in the third scenario, for a 100% demand, was 82.74% less than in the base period. The second scenario was 80.36%, still less than in the base. A comparison of the second and third scenarios shows that the volume change of runoff under climate change (with the same volume

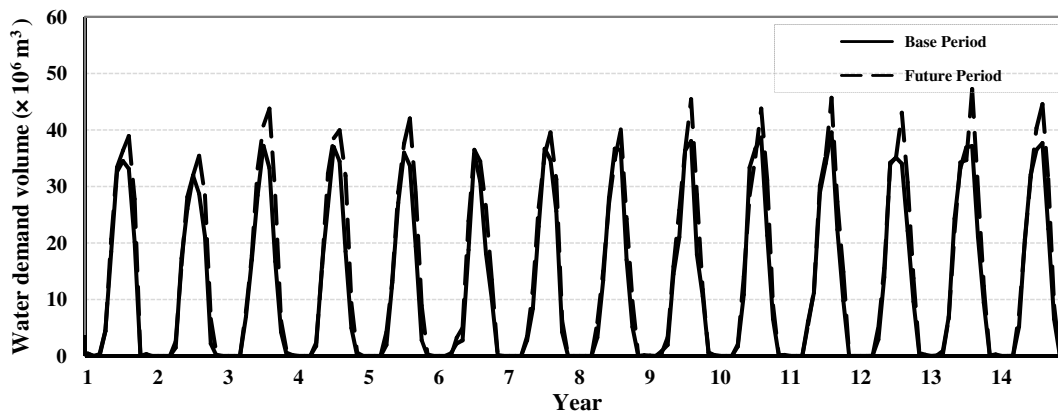


Fig. 8. Annual volume of water demand in base period and future

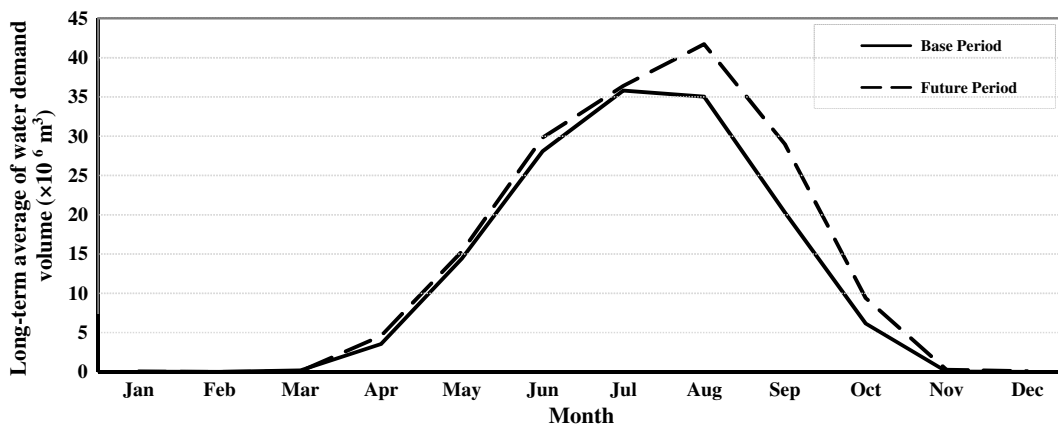


Fig. 9. Long-term average of water demand volume

Table 5. Annual Water Requirement and Water Demand Increase of Aidoghmosh Network in Future Period Relative to Base Period

| Crops | Area under cultivation (ha) | WR_{bas}^a (mm) | WR_{fut}^b (mm) | WR_{fut}/WR_{bas} (mm) | V_{bas}^c ($\times 10^6$ m ³) | V_{fut}^d ($\times 10^6$ m ³) | ΔV ($\times 10^6$ m ³) |
|-----------|-----------------------------|-------------------|-------------------|--------------------------|--|--|---|
| Wheat | 1,620 | 636.88 | 732.95 | 1.15 | 10.32 | 11.87 | 1.56 |
| Barley | 1,080 | 553.59 | 604.93 | 1.09 | 5.98 | 6.53 | 0.55 |
| Alfalfa | 1,620 | 1,422.70 | 1,627.60 | 1.14 | 23.05 | 26.37 | 3.32 |
| Soya | 1,080 | 1,145.21 | 1,288.59 | 1.13 | 12.37 | 13.92 | 1.55 |
| Feed Corn | 675 | 1,155.99 | 1,330.29 | 1.15 | 7.80 | 8.98 | 1.18 |
| Forage | 1,080 | 1,208.19 | 1,405.66 | 1.16 | 13.05 | 15.18 | 2.13 |
| Potato | 1,620 | 1,170.47 | 1,366.20 | 1.17 | 18.96 | 22.13 | 3.17 |
| Walnut | 4,725 | 1,101.80 | 1,304.03 | 1.18 | 52.06 | 61.62 | 9.56 |

^aAnnual water requirement in base period.

^bAnnual water requirement in future period.

^cWater demand volume in base period.

^dWater demand volume in future period.

change of water demand) had a positive influence on the reliability index. This was confirmed in the first scenario for which the volume of demand was constant and the volume of runoff changed; the reliability index under climate change was 86.31%, an improvement of approximately 1% relative to the base period. Thus, it can be concluded that under climate change for the basin, with a fixed volume of water demand, the volume change of runoff increased the reliability index. This is because of the discharge volume distribution uniformity under climate change. Comparisons of

the first and third scenarios indicated that a change in water demand volume decreased the reliability from 86.31 to 82.74%. This is attributable to an increase in water demand under climate change. This was true for 70 and 90% of demand. Results showed that all three scenarios were worse in terms of vulnerability. This worsening was highest in the third scenario and lowest in the first scenario. The vulnerability index in the second and third scenarios was nearly the same and only differed in the amount of runoff volume, showing that a change in runoff volume under climate change had

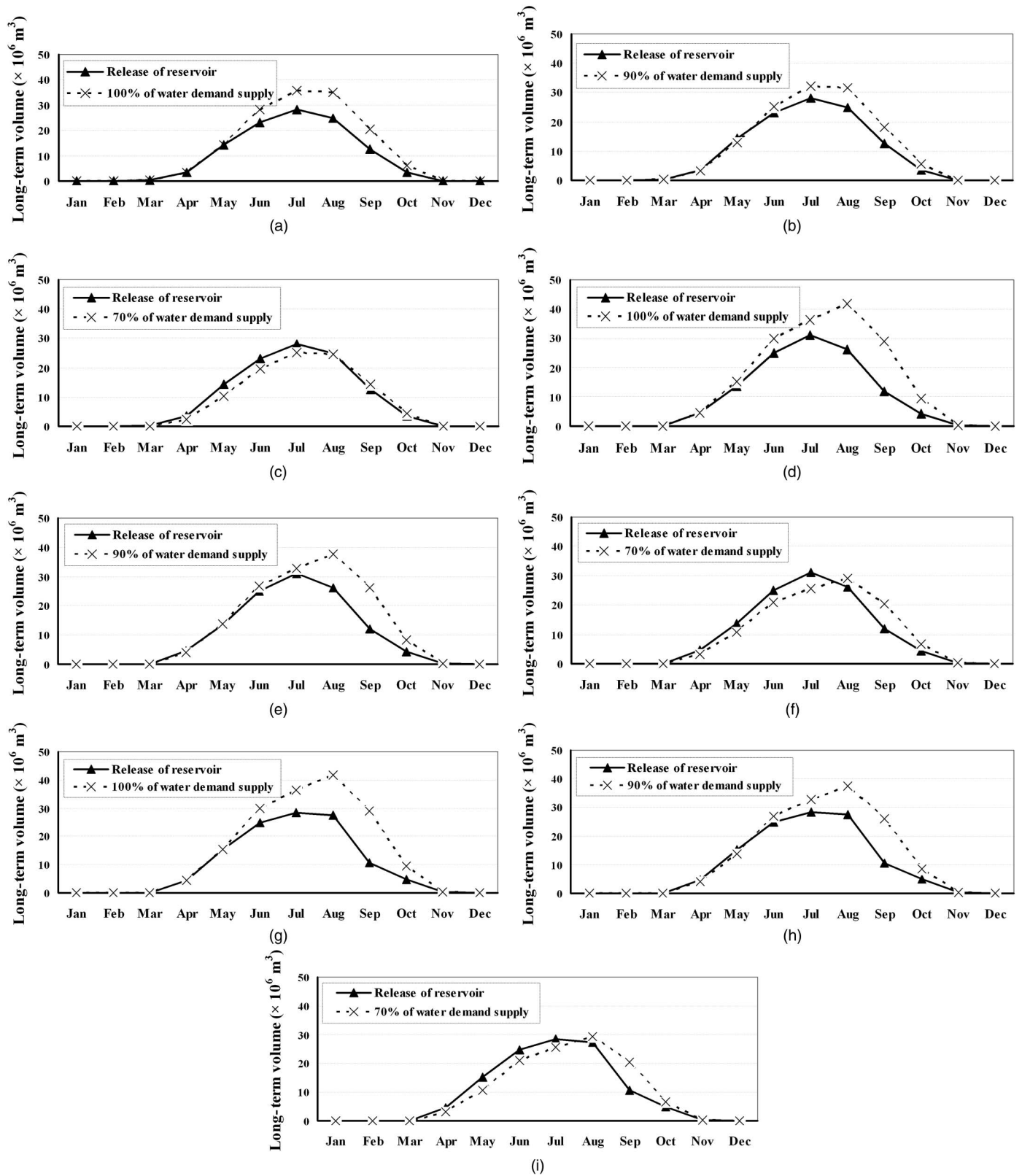


Fig. 10. Release volume of reservoir and volume of water demand in future period: (a), (b), (c) first scenario; (d), (e), (f) second scenario; and (g), (h), (i) third scenario with simulation by WEAP

little effect on this index. Results showed that the resiliency index decreased in all scenarios (except the third scenario) under climate change relative to the base. In addition, a comparison of the first and third scenarios revealed that the water demand volume change

was the primary reason for resiliency improvement. The index values in the second and third scenarios, regarding the difference in runoff volume, indicated that a change in runoff volume was another major factor in improving the resiliency index in the third

Table 6. Comparison of Performance Indexes for Three Scenarios in Base and Future Periods under Simulation and Optimization Approaches

| Indexes | Characteristics of scenarios | | | Base period | | Future period | | Percentage change and indicators situation ^a | | |
|-------------------|------------------------------|----------------------|----------------------|-------------------|------------|---------------|------------|---|------------|--------------|
| | Scenarios | Runoff volume change | Demand volume change | Demand supply (%) | Simulation | Optimization | Simulation | Optimization | Simulation | Optimization |
| Reliability (%) | First | X | | 100 | 85.71 | 57.74 | 86.31 | 63.7 | 0.7 | 10.3 |
| | | | | 90 | 86.31 | 72.02 | 86.31 | 75.0 | 0.0 | 4.1 |
| | | | | 70 | 88.10 | 89.88 | 86.90 | 84.5 | -1.4 | -6.0 |
| | Second | | X | 100 | 85.71 | 57.74 | 80.36 | 56.5 | -6.2 | -2.1 |
| | | | | 90 | 86.31 | 72.02 | 80.95 | 64.9 | -6.2 | -9.9 |
| | | | | 70 | 88.10 | 89.88 | 80.95 | 80.4 | -8.1 | -10.5 |
| | Third | X | X | 100 | 85.71 | 57.74 | 82.74 | 45.8 | -3.5 | -20.7 |
| | | | | 90 | 86.31 | 72.02 | 82.74 | 61.9 | -4.1 | -14.1 |
| | | | | 70 | 88.10 | 89.88 | 82.74 | 80.4 | -6.1 | -10.5 |
| Vulnerability (%) | First | X | | 100 | 21.87 | 26.42 | 23.16 | 26.2 | -5.9 | 0.9 |
| | | | | 90 | 21.32 | 21.77 | 22.70 | 22.1 | -6.5 | -1.5 |
| | | | | 70 | 20.17 | 14.30 | 21.48 | 15.4 | -6.5 | -7.7 |
| | Second | | X | 100 | 21.87 | 26.42 | 29.66 | 33.8 | -35.6 | -27.9 |
| | | | | 90 | 21.32 | 21.77 | 29.13 | 28.9 | -36.6 | -32.8 |
| | | | | 70 | 20.17 | 14.30 | 27.73 | 18.5 | -37.5 | -29.4 |
| | Third | X | X | 100 | 21.87 | 26.42 | 30.23 | 34.5 | -38.2 | -30.6 |
| | | | | 90 | 21.32 | 21.77 | 29.56 | 28.5 | -38.6 | -30.9 |
| | | | | 70 | 20.17 | 14.30 | 27.64 | 19.0 | -37.0 | -32.9 |
| Resiliency (%) | First | X | | 100 | 33.33 | 15.49 | 30.43 | 14.8 | -8.7 | -4.5 |
| | | | | 90 | 34.78 | 19.15 | 30.43 | 19.0 | -12.5 | -0.78 |
| | | | | 70 | 30.00 | 23.53 | 31.82 | 26.9 | 6.1 | 14.32 |
| | Second | | X | 100 | 33.33 | 15.49 | 30.30 | 15.1 | -9.1 | -2.5 |
| | | | | 90 | 34.78 | 19.15 | 28.13 | 18.6 | -19.1 | -2.9 |
| | | | | 70 | 30.00 | 23.53 | 28.13 | 27.3 | -6.2 | 16.0 |
| | Third | X | X | 100 | 33.33 | 15.49 | 34.48 | 17.6 | 3.5 | 13.6 |
| | | | | 90 | 34.78 | 19.15 | 34.48 | 20.3 | -0.9 | 6.0 |
| | | | | 70 | 30.00 | 23.53 | 34.48 | 27.3 | 14.9 | 16.0 |

^aNumbers indicate percentage change of indexes under climate change relative to base period; and sign (+) and (-) indicate increase and decrease in any of the indexes under these conditions, respectively.

scenario under climate change. Thus, for the resiliency, both effects of runoff volume change and water demand volume change were important.

Optimization of Reservoir Performance under Climate Change Scenarios using LINGO

For the optimal operation of the reservoir to supply water, the objective function was considered. Optimal amounts of water release and volume of reservoir storage were calculated by using LINGO for three scenarios. The results are presented in Fig. 11. Because of an increase in demand of 16% and a decrease in inflow volume of 0.7%, the amount of allocation under optimal reservoir management conditions was less than the demand. Similar calculations for 70 and 90% of demand were performed (Fig. 11). As a result, assuming a constant area under cultivation and constant cropping pattern, less irrigation (70% of supply) should be considered for the network under climate change. Other adaptive strategies, such as changes in the levels of cultivation, changes in cropping patterns, greater use of products with lower water requirements, and increases in irrigation efficiency, should be considered.

Table 6 shows values of reliability, vulnerability, and resiliency indexes considering reservoir optimization. The reliability in the third scenario, for 100% water supply, was 45.8% less than in the base. For the second scenario, the index was 56.5%, which was still less than in the base period. For the first scenario in which demand volume was the same and only runoff volume varied, the reliability index was 63.7%, which was 10% better (increase) than in the base period. A comparison of the third and first scenarios

showed that changes in water demand volume caused the reliability to decrease from 63.7 to 45.8%. This is attributable to an increase in water demand under climate change. Therefore, under optimal conditions, the reliability decreased (worsened) (except in the first scenario) relative to the base. This was true for 90 and 70% of water supply. Results also showed that in all scenarios, the vulnerability index under climate change worsened. This decrease in the third scenario was the highest and in the first scenario was the lowest. Vulnerability indexes were nearly the same in the second and third scenarios, which only differed in the amount of runoff volume. Thus, a change in runoff volume had little effect on the index. Also, a comparison of the third and first scenarios showed that water demand volume change was the primary reason for a vulnerability decrease. Thus, under optimal conditions, the vulnerability increased (worsened) in each of the three scenarios relative to the base. In addition, the resiliency index decreased (worsened) in all scenarios under climate change relative to the base period.

Concluding Remarks

This paper investigated the impact of climate change on the performance indexes of the Aidoghmosh Reservoir in Iran, to supply downstream demand in the future (2026–2039) by using a simulation—optimization approach. An investigation of the HadCM3 model showed that the temperature increased (between 0.5 and 2.7°C) and the rainfall varied (-36–76%) in the future compared with the base period. A time series of monthly temperature and rainfall in the future was input to the IHACRES, and a time

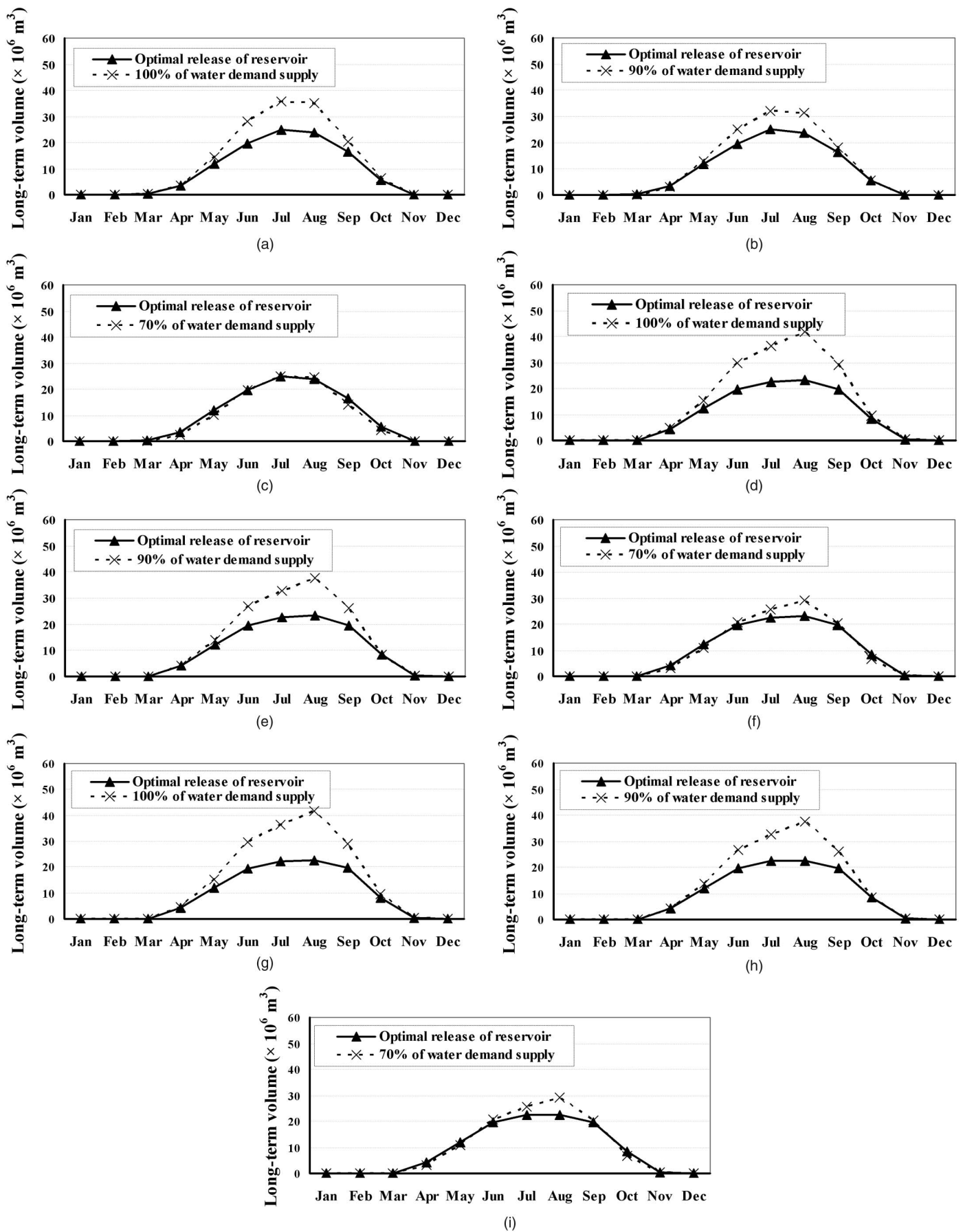


Fig. 11. Release volume of reservoir and volume of water demand in future period: (a), (b), (c) first scenario; (d), (e), (f) second scenario; and (g), (h), (i) third scenario with optimization by LINGO (for 70, 90, and 100% of water demand supply, respectively, in each scenario)

series of monthly runoff was simulated for the future. The results showed that the average long-term annual volume of runoff for the future decreased 0.7% relative to the base. By knowing reference evapotranspiration, obtaining relative humidity in the future, and assuming that wind speed in the future would be similar to that in the base period, values of K_c were calculated. Based on a constant area under cultivation, the water requirement of crops was determined, and water volume was calculated for each month. Water demand volume in the future increased 16% (112×10^6 m³ per year in the base to 130×10^6 m³ in future periods) whereas river runoff volume to the reservoir decreased 0.7% (150.6×10^6 m³ per year in the base to 149.5×10^6 m³ in future periods). To evaluate the reservoir performance in the delivery of water demand volume based on runoff volume of the river, WEAP was used. Reliability, vulnerability, and resiliency indexes for each of the three aforementioned scenarios were then calculated. Results showed that the reliability index decreased (4%) while vulnerability and resiliency indexes increased by 38% and 4%, respectively. The separate effects of each of the parameters of runoff volume and volume of water demand on these indexes showed that a change in runoff volume and water demand volume had positive and little negative influence on the reliability, respectively. For vulnerability, a change in runoff volume had very little negative influence whereas a change in water demand volume had a negative influence. The resiliency index considered the impact of both the volume change in runoff and water demand, and calculations showed that both these parameters had a positive influence on this index. Next, the optimal operation of the reservoir to supply water considered the minimization of the sum of the squares of the deficiencies in each month in the water allocation under climate change conditions. Results showed that in the future relative to the base period, to supply 100% demand for the third scenario, the reliability index decreased (21%) while vulnerability and resiliency indexes increased by 31% and 14%, respectively.

References

- Boyer, C., Chaumont, D., Chartier, I., and Roy, A. G. (2010). "Impact of climate change on the hydrology of St. Lawrence tributaries." *J. Hydrol.*, 384(1–2), 65–83.
- Carter, T. R. (2007). *General guideline on the use of scenario data for climate impact and adaptation assessment*, Finnish Environment Institute, Helsinki, Finland, 39–40.
- Christensen, N. S., Wood, A. W., Voisin, N., Lettenmaier, D. P., and Palmer, R. N. (2004). "The effects of climate change on the hydrology and water resources of the Colorado River basin." *Clim. Change*, 62(1), 337–363.
- Diaz-Nieto, J., and Wilby, R. L. (2005). "A comparison of statistical and climate change factor methods: Impacts on low flows in the River Thames, United Kingdom." *Clim. Change*, 69(2–3), 245–268.
- Doorenbos, J., and Pruitt, W. O. (1984). "Guidelines for predicting crop water requirements." *Irrigation and drainage (FAO), paper 24*, Food and Agricultural Organization of the United Nations, Rome, Italy.
- Intergovernmental Panel on Climate Change (IPCC). (2007). "Climate change 2007: The physical science basis." *Contribution of working group I to the fourth assessment rep. of the intergovernmental panel on climate change*, S. Solomon, D. Qin, M. Manning, Z. Chen, M. Marquis, K. Averyt, M. Tingor, and H. L. Miller, eds., Cambridge Univ. Press, Cambridge, UK.
- IPCC-DDC. (1988). "Data distribution centre." (<http://ipcc-ddc.cru.uea.ac.uk/>).
- Jakeman, A. J., and Hornberger, G. M. (1993). "How much complexity is warranted in a rainfall-runoff model?." *Water Resour. Res.*, 29(8), 2637–2649.
- Knox, J. W., Rodríguez Díaz, J. A., Nixon, D. J., and Mkhwanazi, M. (2010). "A preliminary assessment of climate change impacts on sugarcane in Swaziland." *Agric. Syst.*, 103(2), 63–72.
- LINGO Version 11.0 [Computer software]. LINDO Systems, Chicago.
- Liu, S., et al. (2010). "Crop yield responses to climate change in the Huang-Huai-Hai Plain of China." *Agric. Water Manage.*, 97(8), 1195–1209.
- Loucks, D. P., and Van Beek, E. (2005). "Water resources systems planning and management: An introduction to methods, models and applications." Chapter: Studies and Reports in Hydrology, *Performance criteria*, UNESCO Publishing, Paris, 320–321.
- Muzik, I. (2001). "Sensitivity of hydrologic systems to climate change." *Can. Water Resour. J.*, 26(2), 233–253.
- Purkey, D. R., et al. (2007). "Robust analysis of future climate change impacts on water for agriculture and other sectors: A case study in the Sacramento Valley." *Clim. Change*, 87(Supplement 1), S109–S122.
- Quinn, N. W. T., Brekke, L. D., Miller, N. L., Heinzer, T., Hidalgo, H., and Dracup, J. A. (2004). "Model integration for assessing future hydroclimate impacts on water resources, agricultural production and environmental quality in the San Joaquin Basin, California." *Environ. Model. Software*, 19(3), 305–316.
- Raje, D., and Mujumdar, P. P. (2010). "Reservoir performance under uncertainty in hydrologic impacts of climate change." *Adv. Water Resour.*, 33(3), 312–326.
- Robson, A. J. (2002). "Evidence for trends in UK flooding." *Philos. Trans. R. Soc. London*, 360(1796), 1327–1343.
- Sieber, J., Swartz, C., and Huber-Lee, A. (2005). *User guide for WEAP21*, Stockholm Environment Institute Tellus Institute, Stockholm, Sweden.
- Steele-Dunne, S., et al. (2008). "The impacts of climate change on hydrology in Ireland." *J. Hydrol.*, 356(1–2), 28–45.
- Steinemann, A., and Cavalcanti, L. (2006). "Developing multiple indicators and triggers for drought plans." *J. Water Resour. Plann. Manage.*, 132(3), 164–173.
- Wilby, R. L., and Harris, I. (2006). "A framework for assessing uncertainties in climate change impacts: Low-flow scenarios for the River Thames, UK." *Water Resour. Res.*, 42(2), W02419.
- Xu, C. Y., and Singh, V. P. (2004). "Review on regional water resources assessment models under stationary and changing climate." *Water Resour. Manage.*, 18(6), 591–612.